Why Is Climate Sensitivity So Unpredictable?
Gerard H. Roe, *et al.*
Science **318**, 629 (2007);
DOI: 10.1126/science.1144735

result of global warming, desiccation, land use change (*31*), and re-excavation by increased rates of water erosion (*24*), as well as the dynamics of SOC replacement at sites of erosion. Based on our analysis, we reject both the notion that agricultural erosion substantially offsets fossil fuel emissions and the view that agricultural erosion is an important source of CO_2.

References and Notes

1. R. Amundson, *Annu. Rev. Earth Planet. Sci.* **29**, 535 (2001).
2. A. Bondeau *et al.*, *Glob. Change Biol.* **13**, 679 (2007).
3. A. D. McGuire, *Glob. Biogeochem. Cyc.* **15**, 183 (2001).
4. J. Six, E. T. Elliott, K. Paustian, J. W. Doran, *Soil Sci. Soc. Am. J.* **62**, 1367 (1998).
5. E. A. Davidson, I. L. Ackerman, *Biogeochemistry* **20**, 161 (1993).
6. R. F. Stallard, *Glob. Biogeochem. Cyc.* **12**, 231 (1998).
7. J. W. Harden *et al.*, *Glob. Biogeochem. Cyc.* **13**, 885 (1999).
8. K. Yoo, R. Amundson, A. M. Heimsath, W. E. Dietrich, *Glob. Biogeochem. Cyc.* **19**, 917 (2005).
9. S. V. Smith, R. O. Sleezer, W. H. Renwick, R. Buddenmeier, *Ecol. Apll* **15**, 1929 (2005).
10. S. V. Smith, W. H. Renwick, R. W. Buddenmeier, C. J. Crossland, *Glob. Biogeochem. Cyc.* **15**, 697 (2001).
11. R. Lal, *Environ. Int.* **29**, 437 (2003).
12. P. A. Jacinthe, R. Lal, *Land Degrad. Dev.* **12**, 329 (2001).
13. R. Lal, M. Griffin, J. Apt, L. Lave, M. G. Morgan, *Science* **304**, 393 (2004).
14. Materials and methods are available as supporting material on *Science* Online.
15. T. A. Quine, K. Van Oost, *Global Change Biol.*, Online Accepted Articles, 10.1111/j.1365-2486.2007.01457.x (2007).
16. K. Van Oost *et al.*, *Glob. Biogeochem. Cyc.* **19**, GB4014 (2005).
17. S. G. Liu, N. Bliss, E. Sundquist, T. G. Huntington, *Glob. Biogeochem. Cyc.* **17**, 1074 (2003).
18. N. A. Rosenbloom, J. W. Harden, J. C. Neff, D. S. Schimel, *J. Geophys. Res.* **111 (G1)**, Art. No. G01004 JAN 31 (2006).
19. The proportion of eroded carbon being replaced at the eroding sites ranges from 0.11 to 0.55 when all errors are accounted for (Table 1). Based on radiocarbon studies of density separates (*32*) and bulk fractions (*33*) and on mass weights of SOC fractions (*34*) for globally diverse soils that are not generally eroded, the fraction of SOC that turns over within years to decades varies from 15 to 80%. Eroding sites are less studied, and carbon dynamics may be affected by the introduction of exposed subsoil, which is enriched with less reactive carbon substrates but may also provide nutrients for enhanced plant growth.
20. S. W. Trimble, P. Crosson, *Science* **289**, 248 (2000).
21. We note that burial of SOC in depositional environments has been shown to substantially reduce decomposition (*6*, *9*, *35*) and, therefore, carbon exported beyond watershed boundaries may be assumed to be protected from further decomposition. For our watersheds, the sink term is larger than the carbon export rate (Table 1), which suggests that erosion and deposition induce a sink, irrespective of the fate of the exported carbon.
22. We compared our global results with our high-resolution simulations at various spatial scales and established that our approach provides unbiased and scale-independent estimates of SOC erosion at the continental scale. The range is derived by using the 95% lower/upper confidence level of the replacement term (13 to 45%) using the conservative/extreme model scenario in combination with a low/high global SOC erosion estimate.
23. J. Boardman, *J. Soil Water Conserv.* **53**, 46 (1998).
24. A. Ito, *Geophys. Res. Lett.* **34**, L09403 (2007).
25. Supporting online text.
26. There is also indirect evidence that previous estimates of agricultural erosion are much too high. Estimates using data on river sediment load (*36*) estimated that human activities have led to an increase of ~2 Pg in the global river sediment flux to the ocean (if effects of large dams are omitted). Typical sediment delivery ratios for large basins is on the order of 10% (*11*), that is, an increase in global river sediment flux by 2 Pg should correspond to a global agricultural erosion rate on the order of 20 Pg, which is much more consistent with our estimates.
27. M. M. Bakker, G. Govers, M. D. A. Rounsevell, *CATENA* **57**, 55 (2004).
28. G. W. McCarty, J. C. Ritchie, *Environ. Pollut.* **116**, 423 (2002).
29. The range is obtained by multiplying the low/high global SOC erosion estimates for agricultural land by the average SOC export fraction obtained from our watersheds (30%) (Table 1).
30. K. Lorenz, R. Lal, *Adv. Agron.* **88**, 35 (2005).
31. A. A. Berhe, J. Harte, J. W. Harden, M. S. Torn, *Bioscience* **57**, 337 (2007).
32. S. Trumbore, *Glob. Biogeochem. Cyc.* **7**, 275 (1993).
33. K. Harrison, W. Broecker, G. Bonani, *Glob. Biogeochem. Cyc.* **7**, 69 (1993).
34. A. F. Plante *et al.*, *Eur. J. Soil Sci.* **57**, 456 (2006).
35. J. C. Ritchie, *Water Resour. Bull.* **25**, 301 (1989).
36. J. P. M. Syvitski, C. J. Vorosmarty, A. J. Kettner, P. Green, *Science* **308**, 376 (2005).

37. We thank R. Buddenmeier, S. Billings, A. Nicholas, W. Van Muysen, A. Berhe, and H. Van Hemelrijck for help and advice during the course of this work. Much of this work was supported by the European Commission under the Marie Curie IntraEuropean Fellowship Programme. The contents of this work reflect only the authors' views and not the views of the European Commission. K. Van Oost holds a postdoctoral position at the Fund for Scientific Research Flanders (FWO). J. Six and S. De Gryze were supported by the Kearney Foundation of Soil Science.

Supporting Online Material

www.sciencemag.org/cgi/content/full/318/5850/626/DC1
Materials and Methods
SOM Text
Figs. S1 to S5
Tables S1 to S3
References

29 May 2007; accepted 13 September 2007
10.1126/science.1145724

Why Is Climate Sensitivity So Unpredictable?

Gerard H. Roe* and Marcia B. Baker

Uncertainties in projections of future climate change have not lessened substantially in past decades. Both models and observations yield broad probability distributions for long-term increases in global mean temperature expected from the doubling of atmospheric carbon dioxide, with small but finite probabilities of very large increases. We show that the shape of these probability distributions is an inevitable and general consequence of the nature of the climate system, and we derive a simple analytic form for the shape that fits recent published distributions very well. We show that the breadth of the distribution and, in particular, the probability of large temperature increases are relatively insensitive to decreases in uncertainties associated with the underlying climate processes.

The envelope of uncertainty in climate projections has not narrowed appreciably over the past 30 years, despite tremendous increases in computing power, in observations, and in the number of scientists studying the problem (*1*). This suggests that efforts to reduce uncertainty in climate projections have been impeded either by fundamental gaps in our understanding of the climate system or by some feature (which itself might be well understood) of the system's underlying nature. The resolution of this dilemma has important implications for climate research and policy.

We investigate a standard metric of climate change: Climate sensitivity is defined as the equilibrium change in global and annual mean surface air temperature, ΔT, due to an increment in downward radiative flux, ΔR_f, that would result from sustained doubling of atmospheric CO_2 over its preindustrial value ($2 \times CO_2$). It is a particularly relevant metric for current discussions of industrial emissions scenarios leading to the stabilization of CO_2 levels above preindustrial values (*2*). Studies based on observations, energy balance models, temperature reconstructions, and global climate models (GCMs) (*3*–*13*) have found that the probability density distribution of ΔT is peaked in the range $2.0°C \leq \Delta T \leq 4.5°C$, with a long tail of small but finite probabilities of very large temperature increases. It is important to ask what determines this shape and, in particular, the high ΔT tail, and to what extent we can decrease the distribution width.

Climate consists of a set of highly coupled, tightly interacting physical processes. Understanding these physical processes is a massive task that will always be subject to uncertainty. How do the uncertainties in the physical processes translate into an uncertainty in climate sensitivity? Explanations for the range of predictions of ΔT, summarized in (*14*), have focused on (i) uncertainties in our understand-

Department of Earth and Space Sciences, University of Washington, Seattle, WA 98195, USA.

*To whom correspondence should be addressed. E-mail: gerard@ess.washington.edu

ing of the individual physical processes (in particular, those associated with clouds), (ii) complex interactions among the individual processes, and (iii) the chaotic, turbulent nature of the climate system, which may give rise to thresholds, bifurcations, and other discontinuities, and which remains poorly understood on a theoretical level. We show here that the explanation is far more fundamental than any of these.

We use the framework of feedback analysis (*15*) to examine the relationship between the uncertainties in the individual physical processes and the ensuing shape of the probability distribution of ΔT. Because we are considering an equilibrium temperature rise, we consider only time-independent processes.

Let $\Delta T = \lambda \Delta R_f$, where λ is a constant. In the absence of feedback processes, climate models show $\lambda \equiv \lambda_0 = 0.30$ to 0.31 [K/(W/m^2)] (where λ_0 is the reference climate sensitivity) (*16*), giving an equilibrium increase $\Delta T_0 \approx 1.2$°C in response to sustained $2 \times CO_2$. Because of atmospheric processes, however, the climate sensitivity has a value $\Delta T \neq \Delta T_0$. Conceptually, the forcing ΔR_f produces a temperature change ΔT, which induces changes in the underlying processes. These changes modify the effective forcing, which, in turn, modifies ΔT. We assume that the total change in forcing resulting from these changes is a constant C times ΔT. Thus, $\Delta T = \lambda_0 (\Delta R_f + C\Delta T)$, or

$$\frac{\Delta T}{\Delta R_f} \equiv \lambda = \frac{\lambda_0}{1 - f} \qquad (1)$$

Here, the total feedback factor $f \equiv \lambda_0 C$ (*15*). Clearly, the gain $G \equiv \Delta T/\Delta T_0 > 1$ if $f > 0$, which appears to be the case for the climate system. The range $2°C \leq \Delta T \leq 4.5°C$ corresponds to $1.7 \leq G \leq 3.7$ and $0.41 \leq f \leq 0.73$. Under our definitions, the feedback factors for individual processes are linearly additive, but the temperature changes, or gains, from individual processes are not [see the supporting online material (SOM)].

The uncertainties in measurements and in model parameterizations can be represented as uncertainties in f. Let the average value of f be $\overline{f}$ and let its SD be σ_f, the sum of uncertainties from all the component feedback processes. σ_f can be interpreted in three ways: uncertainty in understanding physical processes, uncertainty in observations used to evaluate $\overline{f}$, and, lastly, inherent variability in the strengths of the major feedbacks. If σ_f is fairly small, we see from Eq. 1 that the uncertainty in the gain, δG, is

$$\delta G \approx \frac{1}{(1 - \overline{f})^2} \sigma_f \equiv (\overline{G})^2 \sigma_f \qquad (2)$$

Thus for $\overline{G} \approx 3$ (corresponding to $\overline{\Delta T} \approx 3.6$°C), uncertainties in feedbacks are magnified by almost an order of magnitude in their effect on the uncertainties in the gain. A second point is that even if σ_f is not large, δG will be large if $\overline{f}$ approaches 1: Uncertainty is inherent in a system where the net feedbacks are substantially positive.

Finally, Eq. 2 shows that it is the sum of all the uncertainties in the feedbacks that determines δG; the uncertainties in the large positive feedbacks are not more important than the others. For example, a compilation of values of the feedback factors extracted from several GCMs (*17*) finds considerable intermodel scatter in the albedo feedback, and although the average magnitude of this feedback is not high, this scatter has an important impact on the uncertainty in the total climate sensitivity.

We now derive the shape of the distribution $h_T(\Delta T)$: the probability density that the climate sensitivity is ΔT. The important

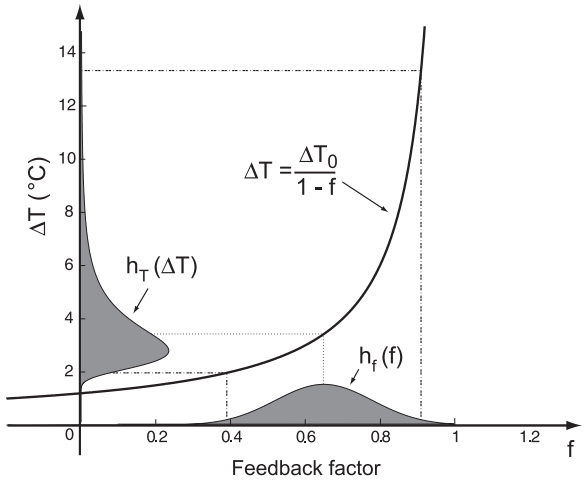

Fig. 1. Demonstration of the relationships linking $h_T(\Delta T)$ to $h_f(f)$. ΔT_0 is the sensitivity in the absence of feedbacks. If the mean estimate of the total feedbacks is substantially positive, any distribution in $h_f(f)$ will lead to a highly skewed distribution in ΔT. For the purposes of illustration, a normal distribution in $h_f(f)$ is shown with a mean of 0.65 and a SD of 0.13, typical to that obtained from feedback studies of GCMs (*17*, *18*). The dot-dashed lines represent 95% confidence intervals on the distributions. Note that values of $f \geq 1$ imply an unphysical, catastrophic runaway feedback.

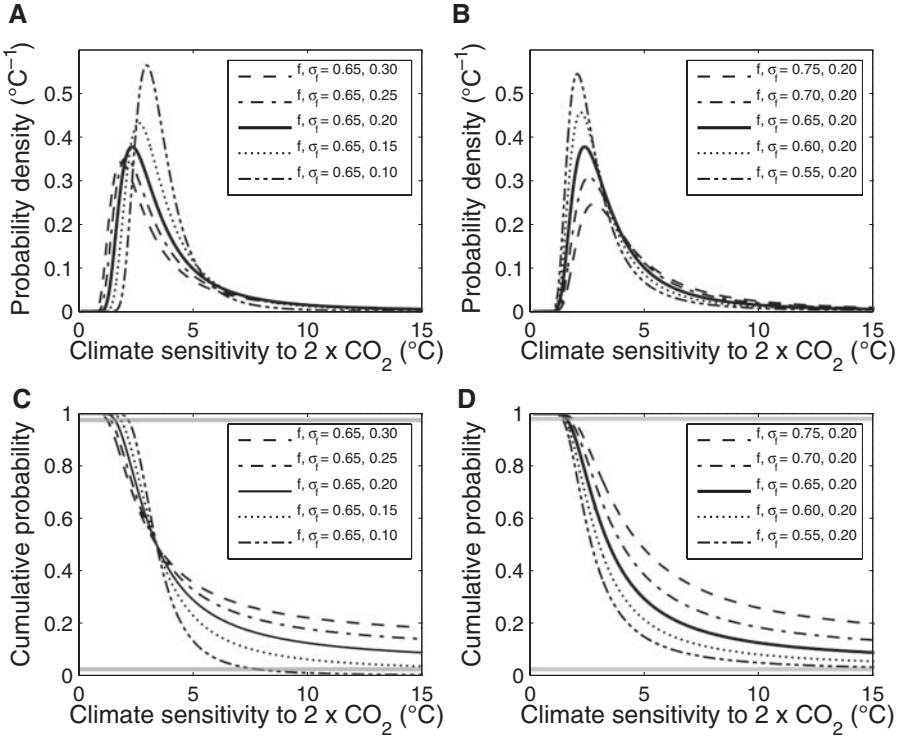

Fig. 2. Probability density distributions (**A** and **B**) and cumulative probability distributions (**C** and **D**) for climate sensitivity, calculated from Eq. 3, for a range of $\overline{f}$ and σ_f. In (C) and (D), the gray lines bound the 95% confidence interval. The peak and the shape of the density distributions are sensitive to both $\overline{f}$ and σ_f only for $\Delta T \leq \approx 5$°C. The cumulative distributions show 50% probability that $\Delta T \geq 1/(1 - \overline{f})$, independent of σ_f, and there is little dependence on σ_f of the probability that $\Delta T > \approx 10$°C. These features of the distributions imply that diminishing σ_f will have a relatively small impact on uncertainties in sensitivity estimates. See also SOM.

features of this distribution are the location of its peak and the shape and extent of the distribution at large ΔT. We focus on the relationships between these features and the parameters of the feedback distribution, $\bar{f}$ and σ_f.

Figure 1 is a schematic picture of the relationships linking $h_T(\Delta T)$ to $h_f(f)$, the probability distribution of f. The reason for the long tail of typical climate sensitivity distributions is immediately evident [see also (*3*)]. Uncertainties in climate processes, and hence feedbacks, have a very asymmetric projection onto the climate sensitivity. As the peak in the $h_f(f)$ distribution moves toward $f = 1$, the probability of large ΔT also grows. The basic shape of $h_T(\Delta T)$ is not an artifact of the analyses or choice of model parameters. It is an inevitable consequence of a system in which the net feedbacks are substantially positive.

Formally, $h_T(\Delta T)$ is related to $h_f(f)$ by the relationship $h_T(\Delta T) = h_f(f(\Delta T))(df/d\Delta T) = \Delta T_0/(\Delta T)^2 h_f(1 - \frac{\Delta T_0}{\Delta T})$. As is commonplace, we assume the errors in the feedback factors are normally distributed: $h_f(f) = (\frac{1}{\sigma_f\sqrt{2\pi}})exp\left[-\frac{1}{2}\left(\frac{(f-\bar{f})}{\sigma_f}\right)^2\right]$. Although the general features of our results do not depend on this assumption, it facilitates our analysis. Then,

$$h_T(\Delta T) = \left(\frac{1}{\sigma_f\sqrt{2\pi}}\right)\frac{\Delta T_0}{\Delta T^2} \times exp\left[-\frac{1}{2}\left(\frac{(1-\bar{f}-\frac{\Delta T_0}{\Delta T})}{\sigma_f}\right)^2\right] \quad (3)$$

Equation 3 shows how uncertainties in feedbacks lead to uncertainty in the response of a system of linear feedbacks. It can be shown that it is algebraically equivalent to a Bayesian derivation of a "posterior" distribution $h(\Delta T)$ based on a uniform previous distribution on feedbacks (SOM). As noted above, several studies have described climate sensitivity distributions similar in form to that indicated in Fig. 1 (*4*–*13*), but the particular power of Eq. 3 is that it provides a simple interpretation of the shape of these distributions. It is also a function that maps uncertainties in feedback processes onto uncertainties in climate sensitivity and therefore permits an analysis of its parametric dependencies. Figure 2 shows $h_T(T)$ and $p_{cum}(\Delta T_c)$, the cumulative probability that the climate sensitivity ΔT will exceed a given threshold, ΔT_c, for a range of values of $\bar{f}$ and σ_f. From Eq. 3, it can be shown that, for all σ_f, half the area under the curve occurs for $\Delta T < \Delta T_{0.5}$. Decreasing either σ_f or $\bar{f}$ concentrates the distribution around $\Delta T = \Delta T_{0.5}$.

The cumulative probability distributions show that decreasing σ_f or $\bar{f}$ steadily reduces the cumulative probability of large climate changes (e.g., $\Delta T \geq 8$°C). However, the probability that ΔT lies in the interval immediately outside the range of the Intergovernmental Panel on Climate Change (IPCC) (say, $4.5°C \leq \Delta T \leq 8°C$) is very insensitive to σ_f and $\bar{f}$ and changes little with ΔT_c. The cumulative probability distributions (Fig. 2, C and D) are driven by the extreme tail of the $h_T(\Delta T)$ distribution, which is a consequence of our choice of a Gaussian for $h_f(f)$. Even if an $h_f(f)$ without an extreme tail is assumed, the probability distributions in the interval beyond the IPCC range remain insensitive to changes in σ_f (SOM).

Thus, foreseeable improvements in the understanding of physical processes, and in the estimation of their effects from observations, will not yield large reductions in the envelope of climate sensitivity. This relative insensitivity of the probability distributions to σ_f is also a likely reason why uncertainty in climate sensitivity estimates has not diminished substantially in the past three decades.

We next compare $h_T(\Delta T)$ from Eq. 3 with selected published distributions of climate sensi-

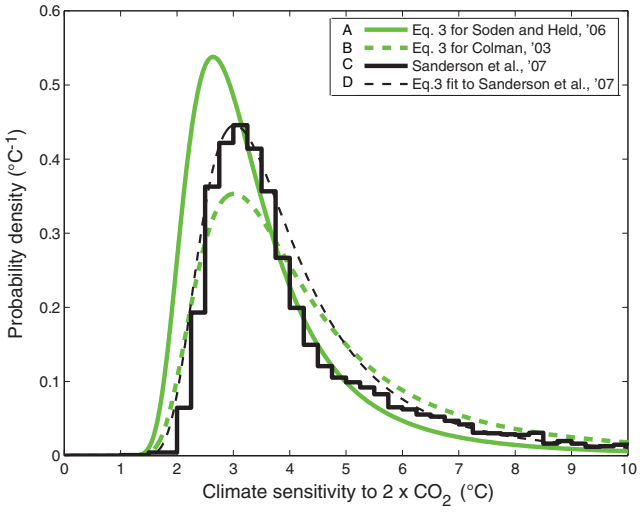

Fig. 3. Climate sensitivity distributions: (**A**) from (*18*), which calculated ($\bar{f}$, σ_f) of (0.62, 0.13) from a suite of GCM simulations; (**B**) from (*17*), which found ($\bar{f}$, σ_f) of (0.7, 0.14) from a different suite of models; and (**C**) from the ~5700-member multiensemble climateprediction.net (*9*, *10*) for different choices of cloud processes. [Data were provided courtesy of B. M. Sanderson] (**D**) Fit of Eq. 3 to the result of (*10*), which was found by estimating the mode of the probability density and its accompanying ΔT and solving for ($\bar{f}$, σ_f) from Eqs. 2 and 3, which yielded values of (0.67, 0.12).

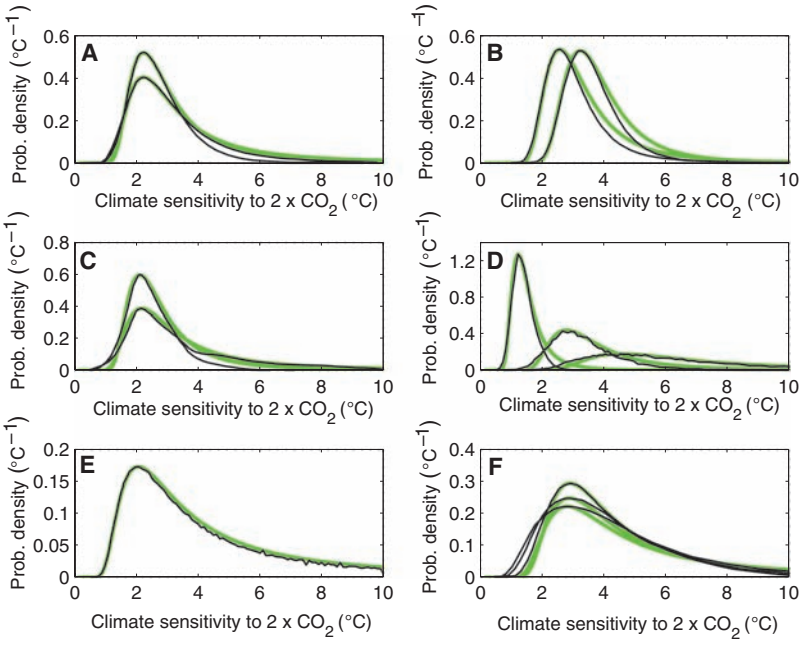

Fig. 4. Climate sensitivity distributions from various studies with the use of a wide variety of methods (black lines) and overlain with a fit of Eq. 3 (green lines), as described in Fig. 3: (**A**) from (*11*), fit with ($\bar{f}$, σ_f) = (0.58, 0.17) and (0.63, 0.21); (**B**) from (*8*), fit with ($\bar{f}$, σ_f) = (0.67, 0.10) and (0.60, 0.14); (**C**) from (*6*), fit with ($\bar{f}$, σ_f) = (0.64, 0.20) and (0.56, 0.16); (**D**) from (*4*), fit with ($\bar{f}$, σ_f) = (0.82, 0.11), (0.65, 0.14), and (0.15, 0.28); (**E**) from (*5*), fit with ($\bar{f}$, σ_f) = (0.86, 0.35) [see also (*29*)]; and (**F**) from (*12*), fit with ($\bar{f}$, σ_f) = (0.72, 0.17), (0.75, 0.19), and (0.77, 0.21).

tivity. Figure 3 shows a distribution, determined from the multi-ensemble climateprediction.net experiment, for different representations of several cloud processes (*9*, *10*). Independent estimates of feedback parameters for two different suites of GCMs (*17*, *18*) determine values for ($\overline{f}$, σ_f) of (0.70, 0.14) and (0.62, 0.13), respectively (*19*). We calculate the implied climate sensitivity distributions from Eq. 3. These match the numerically derived distributions of (*10*) quite well. We obtained a closer match by solving Eq. 3 for the $\overline{f}$ and σ_f that effectively characterize the feedback processes within the model used by (*9*, *10*) and used these parameters to generate the distribution.

Fits to several other published distributions (obtained by a wide variety of techniques), shown in Fig. 4, are also quite successful, with values $0.15 \leq \overline{f} \leq 0.86$ and $0.10 \leq \sigma_f \leq 0.35$. Some differences are seen, especially in the tail of the distributions. This is to be expected because some studies explicitly analyze the non-Gaussian distribution of uncertainties in the physics and various a priori assumptions. Nonetheless, all of these published distributions are, to a good approximation, consistent with propagation of physical-process uncertainties in a simple system of linear feedbacks.

The shape of $h_T(\Delta T)$, including its tail, is crucially dependent on the magnitude of $\overline{f}$, which we have assumed is independent of ΔT. Is there any chance that, as warming continues, the probability of extreme values of ΔT will actually diminish? This might result if the feedback factors are functions of temperature. We have performed a preliminary analysis of the changes in the $h_T(\Delta T)$ distribution that would result from adding nonlinear terms in the Stefan-Boltzmann and water vapor feedbacks (SOM). This analysis shows that these second-order effects are equivalent to decreasing $\overline{f}$ by about 0.01 to 0.02, the small effect of which can be gauged from the curves in Fig. 2. To remove the skewness completely would require changes in feedback strength that are about 25 times as great (SOM). Several nonlinear interactions of this strength might, however, contribute an additional $\sigma_f \sim 0.1$, which would change the particulars of a given probability distribution but not its fundamental characteristics. The identification and quantification of these nonlinear interactions are enormously harder tasks than the analysis of the linear feedbacks. It may be that a practical limit to the predictability of climate sensitivity should be anticipated.

It is tempting to speculate on what we can learn about the extreme tail of $h_T(\Delta T)$ from paleoclimate data. For instance, Eq. 3 can be extended to evaluate how uncertainties in reconstructions of past temperatures and net radiative forcing propagate to uncertainties in feedback strengths. Moreover, the data that we have on extreme climates [for example, the Eocene warmth and Proterozoic "snowball Earth" (*20*, *21*)] suggest that the climate system may have been acutely sensitive to radiative forcing during some intervals of Earth's history. Our results imply that dramatic changes in physical processes are not necessary for dramatic changes in climate sensitivity, provided that those changes in processes can all align in the same direction toward increased sensitivity. These are events of low but not zero probability.

Despite the enormous complexity of the climate system, the probability distribution of equilibrium climate sensitivity is well characterized by Eq. 3, which reflects the straightforward, compounding effect of essentially linear feedbacks and depends on only the two parameters $\overline{f}$ and σ_f. We have shown that the uncertainty in the climate sensitivity in $2 \times CO_2$ studies is a direct and general result of the fact that the sum of the underlying climate feedbacks is substantially positive. Our derivation of $h_T(\Delta T)$ did not depend on nonlinear, chaotic behavior of the climate system and was independent of details in cloud and other feedbacks. Equation 3 appears to explain the range of climate sensitivities reported in previous studies, which are well synthesized by the IPCC (*1*). Furthermore, reducing the uncertainty in individual climate processes has little effect in reducing the uncertainty in climate sensitivity. We do not therefore expect the range presented in the next IPCC report to be greatly different from that in the 2007 report. On the basis of the values of $\overline{f}$ and σ_f compiled from our analysis of a large number of published results, it is evident that the climate system is operating in a regime in which small uncertainties in feedbacks are highly amplified in the resulting climate sensitivity. We are constrained by the inevitable: the more likely a large warming is for a given forcing (i.e., the greater the positive feedbacks), the greater the uncertainty will be in the magnitude of that warming.

References and Notes

1. S. Solomon *et al.*, Eds. *Climate Change 2007: The Physical Science Basis. Contribution of Working Group I to the Fourth Assessment Report of the Intergovernmental Panel on Climate Change* (Cambridge Univ. Press, 2007).
2. Climate sensitivity is a measure of equilibrium climate change. During the adjustment to the new equilibrium, time-dependent factors, in particular ocean heat uptake, are also important.
3. M. R. Allen *et al.*, in *Avoiding Dangerous Climate Change*, H. J. Schellnhuber, W. Cramer, N. Nakicenovic, T. Wigley, G. Yohe, Eds. (Cambridge Univ. Press, 2006), pp. 281–289.
4. N. G. Andronova, M. E. Schlesinger, *J. Geophys. Res.* **106**, 22605 (2001).
5. J. M. Gregory, R. J. Stouffer, S. C. B. Raper, P. A. Stott, N. A. Rayner, *J. Clim.* **15**, 3117 (2002).
6. C. E. Forest, P. H. Stone, A. P. Sokolov, M. R. Allen, M. D. Webster, *Science* **295**, 113 (2002).
7. D. J. Frame *et al.*, *Geophys. Res. Lett.* **32**, L09702 (2005).
8. J. M. Murphy *et al.*, *Nature* **430**, 768 (2004).
9. D. A. Stainforth *et al.*, *Nature* **433**, 403 (2005).
10. B. M. Sanderson, C. Piani, W. J. Ingram, D. A. Stone, M. R. Allen, *Clim. Dyn.* published online 3 July 2007; 10.1007/s00382-007-0280-7, in press.
11. G. C. Hegerl, T. J. Crowley, W. T. Hyde, D. J. Frame, *Nature* **440**, 1029 (2006).
12. D. L. Royer, R. A. Berner, J. Park, *Nature* **446**, 530 (2007).
13. C. Piani, D. J. Frame, D. A. Stainforth, M. R. Allen, *Geophys. Res. Lett.* **32**, L23825 (2005).
14. S. Bony *et al.*, *J. Clim.* **19**, 3445 (2006).
15. There are ambiguities surrounding feedback terminology in the climate literature. Hansen *et al.* (*22*) reversed the definition of feedback factor and gain from what is conventional in electronics (*23*–*25*). The convention adopted by Hansen *et al.* (*22*) has permeated much, but not all, of the climate literature [compare with (*26*–*28*)]. For the standard electronics definitions, it can be shown that the feedback factor is proportional to the fraction of the system response fed back into the system input and that the gain is the proportion by which the output has gained (i.e., been amplified) by the inclusion of the feedbacks. In this study, we retain the traditional electronics definitions. See also the SOM.
16. In climate models, λ_0 is found by calculating the climate response to forcing, allowing only surface temperature to change (*17*, *18*, *22*).
17. R. Colman, *Clim. Dyn.* **20**, 865 (2003).
18. B. J. Soden, I. M. Held, *J. Clim.* **19**, 3354 (2006).
19. Researchers (*17*, *18*) estimated mean and SD of feedback factors calculated from two different suites of climate models. First, Colman (*17*) found a mean and SD of (0.11, 0.06) for the albedo feedback factor; (0.17, 0.11) for the cloud feedback factor; and (0.42, 0.06) for the water vapor and lapse rate feedbacks combined. Second, Soden and Held (*18*) found a mean and SD of (0.09, 0.02) for the albedo feedback factor; (0.22, 0.12) for the cloud feedback factor; and (0.31, 0.04) for the water vapor and lapse rate feedbacks combined. The water vapor and lapse rate feedbacks are typically combined because models show a strong negative correlation between the two. Although the combined feedback for water vapor and lapse rate has the largest magnitude, the greatest contributor to uncertainty is the cloud feedback.
20. P. F. Hoffman, D. P. Schrag, *Terra Nova* **14**, 129 (2002).
21. L. C. Sloan, D. K. Rea, *Palaeogeogr. Palaeoclimatol. Palaeoecol.* **119**, 275 (1996).
22. J. E. Hansen *et al.*, in *Climate Processes and Climate Sensitivity*, J. E. Hansen, T. Takahashi, Eds. (Geophysical Monograph 29, American Geophysical Union, Washington, DC, 1984), pp. 130–163.
23. H. W. Bode, *Network Analysis and Feedback Amplifier Design* (Van Nostrand, New York, 1945).
24. R. Kories, H. Schmidt-Walter, *Electrical Engineering: A Pocket Reference* (Springer, Berlin, 2003).
25. J. G. Graeme, *Optimizing Op-Amp Performance* (McGraw-Hill, New York, 1997).
26. National Research Council, *Understanding Climate Change Feedbacks* (National Academies Press, Washington, DC, 2003).
27. R. S. Lindzen, M.-D. Chou, A. Y. Hou, *Bull. Am. Meteorol. Soc.* **82**, 417 (2001).
28. J. M. Wallace, P. V. Hobbs, *Atmospheric Science: An Introductory Survey* (Academic Press, San Diego, ed. 2, 2006).
29. The curve from (*5*) is a numerical calculation from climate observations and uses an equation isomorphic to Eq. 3.

30. We thank P. Guttorp, J. M. Wallace, D. Hartmann, D. Battisti, C. Bretherton, E. Steig, D. Stolar, and S. Warren for insightful comments on drafts of the manuscript; M. R. Allen, M. Cane, and one anonymous reviewer for constructive suggestions that substantially improved the manuscript; and H. J. Smith, the editor. G.H.R. thanks Yale University for support as a Flint Visiting Professor.

Supporting Online Material

www.sciencemag.org/cgi/content/full/318/5850/629/DC1
SOM Text
Fig. S1
References

7 May 2007; accepted 14 September 2007
10.1126/science.1144735